Rheological Study on Tetrafluoroethylene/ Hexafluoropropylene Copolymer and Its Implication For Processability

Xiao-Yong Chen,[1,2] Wang Zhang Yuan,[1] Hong Li,[1] Yongming Zhang[1]

[1]*School of Chemistry and Chemical Engineering, Shanghai Jiao Tong University, Shanghai 200240, China*
[2]*School of Materials Science and Engineering, North University of China, Taiyuan 030051, China*

Received 26 April 2011; accepted 20 September 2011
DOI 10.1002/app.35665
Published online in Wiley Online Library (wileyonlinelibrary.com).

ABSTRACT: Tetrafluoroethylene/hexafluoropropylene copolymers (FEPs) are widely used in diverse fields due to their outstanding performances in chemical resistance, thermal stability, and insulation. However, their processsability is poor, exhibiting narrow stable flow region and remarkably early melt fracture. Herein, we tried to explore the origin of such poor processability in a rheological way, because melt rheology behaviors are highly related to their processing processes. The shear rheology results indicate that FEPs exhibit multiple flow regions. The flow curve of FEP608 was obtained, and its η_0 value was calculated to be 1.70 kPa s^{-1} at 360°C. Extensional rheological data suggest that FEPs have much lower *e* and *B* values when compared with those of common polymers, suggesting their weaker elasticity during extrusion. Based on such rheological results, the poor processability of FEPs is ascribed to their high viscosity induced by special interchain interaction associating with F atom, which can easily cause accumulated elastic energy.
 J Appl Polym Sci 000: 000–000, 2012

Key words: FEP; shear viscosity; extensional rheology; melt elasticity; processability

INTRODUCTION

Fluoropolymers are receiving increasing attentions due to their unique properties, such as wonderful thermal, chemical, aging, and weather resistance, oil and water repellency, low flammability, low refractive index and dielectric constant, outstanding inertness and biocompatibility, and so forth. Such excellent properties render them suitable for a variety of applications in coatings, electronic materials, petrochemical and automotive industries, chloro-alkali industry, fuel cells, aerospace and aeronautics, optics, treatment of textiles, and so on. Among diverse fluoropolymers, tetrafluoroethylene (TFE)/ hexafluoropropylene (HFP) copolymers (FEPs) have attracted considerable attentions due to their outstanding chemical resistance, wide service temperature range, excellent thermal stability, and promising insulation properties. Nowadays, there are increasing commercial interests in FEPs, and thus, the resin is being widely used in many harsh conditioned areas, such as aircraft hookup wire, shield against strong acid and base, advanced composites in aerospace and ocean applications.[1–6]

Particularly, FEPs have lower melting temperature and melting viscosity than those of polytetrafluoroethylene (PTFE), making them capable of being melt-processed. However, their processability is poor, exhibiting terribly narrow stable shear flow and remarkably early melt fracture. Considering their tremendous applications, further exploring of such attribute of FEPs is thus essential. It is known that rheological behaviors of polymer melts are closely related to their processing processes. Rheological parameters of the melts provide valuable information for the optimization of processing conditions to obtain high quality products. Nevertheless, researches on rheological behavior and processability of FEPs are few. Wu[7] and Tuminello[8] estimated the molecular weight distribution of FEP based on dynamical rheological characterization. Koyama et al. reported the effects of prethermal history and addition of PTFE on dynamic shear and elongational flow behaviors of FEP near crystal melting transition under low extensional strain rate.[9,10] Rosenbaoum et al.[5,11–13] determined stable shear flow characteristics of FEP using a capillary rheometer and confirmed its narrow steady flow region.

However, up to date, studies on illuminating the nature of narrow processing window of FEPs using rheological methods are scarcely found. We even

Correspondence to: Y. Zhang (ymzsjtu@yahoo.com.cn).
Contract grant sponsor: "11th 5-year" National Key Technologies R&D Program of China; contract grant number: 2006BAE02A04.
Contract grant sponsor: Shanghai Leading Academic Discipline Project; contract grant number: B202.

cannot find any works on extensional rheological behaviors of pure FEPs under high deformation rates, although it is important in blow molding and tape casting. In practice, besides shear flow, elongational deformation also plays an important role in wire coating processing of FEPs.[10] Meissner-type uniaxial tensile rheometer[10,14] can achieve true and pure extensional properties. However, this technique can only effectively characterize extensional flow behavior at low strain rate and is difficult to operate. Alternatively, capillary rheometer with a set of dies can be used to determine elongational viscosity on the basis of Cogswell and Binding's work on converging flow and entry flow.[15–18] Such technique is easy to operate, needs no extra instruments, and has relatively better accuracy, especially at high elongational strain rate.[19–23] Moreover, capillary rheometry can also provide information about elasticity, such as melt fracture phenomena and entrance pressure drops of the capillary die. Subsequently, the elastic parameters such as recoverable strain, normal stress, and shear modulus can be calculated. Thus, the effect of elasticity of FEP on processability can be further derived.[24–28]

Taking into account of the fundamental significance and technical implication, herein, we tried to shed light on the origin of poor processability of FEPs through rheological study, which is an effective tool for optimizing polymer processing conditions and polymer-based devices design. In this article, we examined and modeled the rheological performance, particularly extensional rheology behavior of FEPs, evaluated their elasticity, and further revealed the origin of their poor processability.

THEORY AND EXPERIMENTAL

Carreau Model

Carreau model, which could predict zero shear viscosity η_0, as shown in eq. (1), is used to fit the experimental data and predict the flow behavior of FEP.

$$\eta_s = \eta_0[1 + (\lambda\dot{\gamma})^2]^{\frac{n-1}{2}}, \quad (1)$$

where η_s, λ, $\dot{\gamma}$, and n are shear viscosity, relaxation time, shear rate, and non-Newtonian index, respectively.[25]

Cogswell's Extensional Rheology Theory Based on Entry Flow

When a fluid flow from the barrel of a capillary rheometer into a capillary die, converging flow occurs, and the fluid is stretched at the die entrance along the direction of its axis. The stretching brings to extra pressure drops (ΔP_{ent}) localized at the entry of the die.[15–18] The converging flowing is a complex flow, which combines extensional with shear flow component. Given the shear flow behavior of the material, in principle, the extensional viscosity (η_e) can be deduced from ΔP_{ent}. η_e, extensional stress (σ_e), and extensional rate ($\dot{\varepsilon}$) could be determined as follows,

$$\eta_e = \left[\frac{3(n+1)\cdot\Delta P_{ent}}{4\sqrt{2}\cdot\dot{\gamma}}\right]^2 \cdot \frac{1}{\eta_s} \quad (2)$$

$$\sigma_e = \frac{3(n+1)\cdot\Delta P_{ent}}{8} \quad (3)$$

$$\dot{\varepsilon} = \frac{\dot{\gamma}}{2}\sqrt{\frac{2\eta_s}{\eta_e}} \quad (4)$$

The corresponding extensional rate is averaged over the strain rates experienced by the fluid in the converging flow, and it is found that η_e calculated via the entry flow method show good accurateness compared with those obtained from other absolute methods.[20,22]

Experimental

Three FEP granular resins with different molecular weights, FEP600A, FEP600B, and FEP608, were supplied by Dongyue Group, China. Their melt indexes are 2.7, 7.5, and 18.8 g/10 min, respectively, under 350°C and 5 kg weight load giving the molecular weights (MWs) in the order of $MW_{FEP600A} > MW_{FEP600B} > MW_{FEP608}$. Defined MWs, however, could not be determined due to the insolubility of FEPs in common solvents. HFP content is $\sim$ 12.8 mol %. All rheological tests were performed in a twin-barrel capillary rheometer, RH10 (Malvern Instruments, UK). The shear rheological experiments were conducted from 20 to 2100 s^{-1} at 310, 335, and 360°C, respectively. Although 20 s^{-1} is the lower boundary of shear rate which the rheometer could provide trustable measurement, a shear rate of 2100 s^{-1} is enough for exploring all flow regimes of FEP extrusion. Meanwhile, FEPs can be processed in the temperature range of 310 $\sim$ 360°C, wherein FEP melts possess suitable viscosity without decomposition or melting partially. Three measurements were taken to evaluate the data reproducibility, and acceptable results were obtained within the tolerance of 5%. Circular dies were used with a diameter of 1 mm, entrance angle of 180° and length to diameter ratio (l/d) of 16. All FEPs were dried at 120°C for 2 h before tests. The die swell measurements were conducted by Vernier caliper with a 1 cm long extrudate for at least five times. Effect of gravity on die swell was neglected. Surface images of FEP melt extrudates were taken by a common digital single lens reflex camera (NIKON D40, Japan).

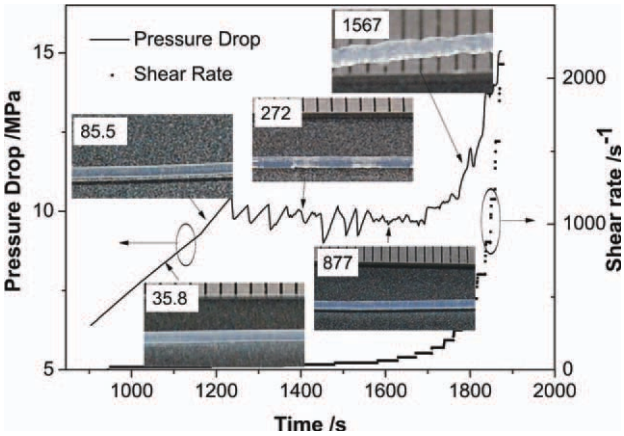

Figure 1 Real time pressure drop data of FEP608 335°C and representative photos of surface texture of FEP608 extrudates from steady region, sharkskin region, stick-slip region, superextrusion region, and gross distortion region at the shear rates of 35.8, 85.5, 272, 877, and 1568 s^{-1}, respectively. [Color figure can be viewed in the online issue, which is available at wileyonlinelibrary.com.]

RESULTS AND DISCUSSION

Flow Instability of FEPs

As shear rate $\dot{\gamma}$ increases during extrusion, FEP melt could be divided into five regions, namely, stable region, sharkskin region, stick-slip region, superextrusion region, and gross distortion region. Figure 1 shows the real time pressure drop data and the corresponding typical pictures of FEP extrudates from the five different flow regions. Obviously, the surfaces of extrudates from stable and superextrusion regions are quite smooth, whereas those from sharkskin, stick-slip, and gross distortion regions are coarse. Rosenbaoum et al.[5,29,30] also reported the presence of five flow regions during FEP extrusion. The real time data are quite different from each other under varying flow regions. For example, pressure drop increases monotonously in steady region but oscillates in stick-slip region. Such multiple flow regions were also found in many conventional polymers during capillary extrusion, such as polyethylene (PE),[31–34] polypropylene (PP),[33,35–39] polybutadiene,[40] and so on.

The onset shear rates and critical shear stresses of various regions for three FEPs are listed in Table I. No steady-stable flow region could be observed for FEP600A at 310 and 335°C, and for FEP600B at 310°C, during tested $\dot{\gamma}$ region due to their high viscosities and MWs. Apparently, compared with common polymers such as PE and PP, the steady-state flow region of FEP like FEP608 is quite narrow with $\dot{\gamma}$ below 85.5 s^{-1} at 335°C. However, the critical shear stresses of FEP capillary extrusion are nearly 0.2 MPa, which is approaching those of PE and PP.[31–39] The reason for the remarkable stresses under such low shear rates will be discussed later. Meanwhile, it is found that increasing MW or decreasing processing temperature can induce earlier melt fracture, and thus more deteriorated processing performance. Because of the narrow stable flow regions, FEP resins are labeled with poor processability.

Plots of apparent shear stress (τ) versus $\dot{\gamma}$ are used to characterize flow instabilities of FEP, and the results are shown in Figure 2. When a melt fracture happens, the plots will break and become discontinuous. Processing temperature (T_p) and MW play important roles in extrusion stabilization of FEP. Steady flow regions become wider and shift to higher shear rates with higher T_p or lower MW. Other four flow regions will also alter with changes in T_p or MW. Because of hysteresis, the transition $\dot{\gamma}$ from steady flow region to stick-slip region is higher than that observed by eyes (Table I). It is noted that the $\tau \sim \dot{\gamma}$ curves crossover each other [Fig. 2(A)] at various T_p. Similar phenomenon was also observed by Rosenbaum.[5] Such crossovers can occur because the critical wall shear stress increases with increasing temperature. When the temperature is decreased, the onset melt fracture occurs at much smaller apparent shear rates and wall shear stresses, and thus much lower viscosity. Consequently, the shear viscosity under evaluated temperatures shifts to higher values in stable flow regions, thus giving crossovers in the flow curves. For example, at 85.5 s^{-1} and

TABLE I
Onset Shear Rates and Stresses of Various Flow Regions of FEPs at Different Processing Temperatures

		Sharkskin		Stick-slip		Superextrusion		Gross distortion	
Resins	T_p (°C)	$\dot{\gamma}_c$ (s^{-1})	σ_c (MPa)	$\dot{\gamma}_c$ (s^{-1})	σ_c (MPa)	$\dot{\gamma}_c$ (s^{-1})	σ_c (MPa)	$\dot{\gamma}_c$ (s^{-1})	σ_c (MPa)
FEP600A	360	35.7	0.165	85.5	0.233	365	0.242	654	0.244
FEP600B	335	35.7	0.160	85.5	0.203	489	0.214	877	0.223
	360	64	0.186	154	0.248	654	0.273	1170	0.266
FEP608	310	47.8	0.145	85.5	0.194	364.7	0.188	877	0.195
	335	85.5	0.167	154	0.236	877	0.249	1568	0.247
	360	154	0.200	202	0.251	1170	0.302	2096	0.295

$\dot{\gamma}_c$, critical shear rates where polymer extrusion mechanism changes take place; σ_c, critical shear stress where polymer extrusion mechanism changes take place.

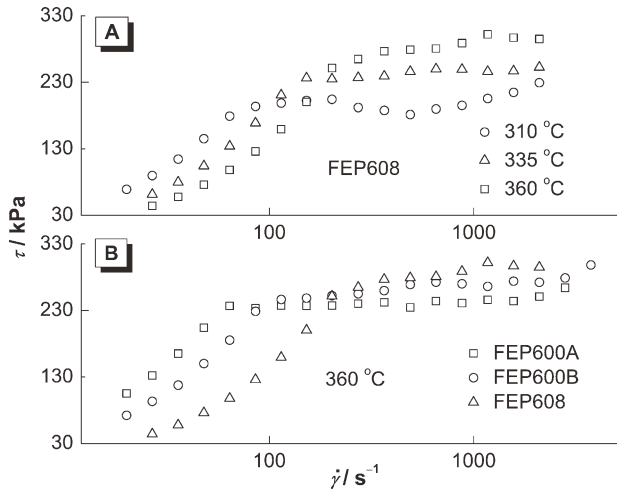

Figure 2 Effects of (A) processing temperature T_p and (B) molecular weight on apparent flow curves of FEPs.

335°C, mild melt surface tearing happens for FEP608 and the wall shear stress starts to decrease. However, at 360°C, the melt is still in stable state and the wall shear stress increases continually as $\dot{\gamma}$ increases. Subsequently, apparent shear viscosity η_s at 335°C is lower than that at 360°C. Changes of MW can also lead to variations in the onset shear rate of melt distortions, thus giving the appearance of crossovers for $\tau \sim \dot{\gamma}$ curves [Fig. 2(B)].

The Flow Curve

Polymer melt viscosity reflects inherent resistance of flow and plays an important role in polymer processing. Flow curve of $\eta_t \sim \dot{\gamma}_t$ (where η_t and $\dot{\gamma}_t$ represent true shear viscosity and true shear rate, respectively) helps choose suitable extrusion velocity in resins extrusion processing and is widely used in polymer industries.

The true shear viscosity and true shear rate were calculated and plotted using Bagley and Rabinowitch correction. The true $\eta_t \sim \dot{\gamma}_t$ curves of three FEPs at different temperatures within steady flow region are shown in Figure 3. Shear viscosity of FEP is at the same order of magnitude, but higher than that of some common polymer, such as PE, PP, and PS,[24,33,35,37–38,41] and far lower than that of PTFE (usually, the shear viscosity of PTFE is several MPa s^{-1}[42]). It endows FEP resin better processability than PTFE and makes it one of the most extensively applied fluoropolymers. When compared with common polymers, FEP still needs more power to process due to its high shear viscosity. Remarkable shear-thinning phenomenon would be observed for all FEPs at different temperatures with η_t located between 1 and 10 kPa s^{-1}. FEP600A with the highest MW possesses the highest η_t and the narrowest steady flow region. Higher MW results in higher viscosity due to the increase of physical entanglement points, poorer chain mobility, and smaller free volume.[25]

Generally speaking, rheological characterization is conducted within limited deformation rate range, and thus simulation based on flow model is adopted frequently for more extensive rheological information beyond the experimental range. Carreau model is often used to fit the experimental data and predict the flow behavior of polymers.[43–45] Herein, it is also utilized and a good fit to the flow curve of FEP608 at 360°C is obtained, as can be seen from Figure 3. The zero shear viscosity (η_0), relaxation time (λ), and non-Newtonian index (n) are calculated to be 1.70 kPa s^{-1}, 0.019 s, and 0.79, respectively. Such η_0 value is close to that of Group B (a TFE/HFP copolymer with a weight ratio of 85/15, similar to the samples examined herein) calculated from rotational rheological data in Rosenbaoum's study.[5]

Extensional Viscosity

Koyama et al.[9–10] reported the extensional viscosity of pure FEPs under extremely low stretch rate (not larger than 1 s^{-1}). In practice, the processing takes place at high deformation rates. Although it is still controversial that whether extensional viscosity measurement based on entry flow method is an effective and convenient way to obtain useful processing parameters, the technique is frequently used to analyze various flows such as contracting flows in capillary dies[28,33,35,46] and works well. Extensional viscosity (η_e) could be extracted even at relatively low pressure drop about 0.1 ~ 0.2 MPa in orifice die.

Figure 4 presents η_e of FEP608 as a function of extensional stress (σ_e), where "tension-thinning"[47] could be observed at all test temperatures. Clearly, η_e decreases with increasing σ_e. Such tension-

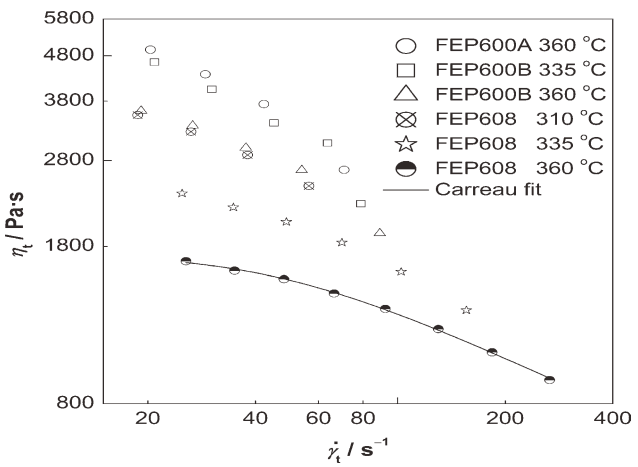

Figure 3 Plots of true shear viscosity versus true shear rate for three FEPs at different temperatures.

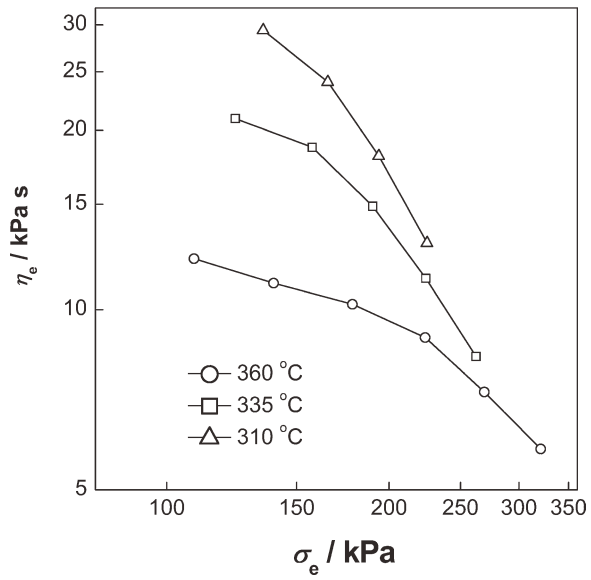

Figure 4 Plots of extensional viscosity versus extensional stress for FEP608 at different temperatures.

thinning behavior could be explained in terms of disentanglement of macromolecular chains at high stretching rate.[26,45] Tension-thinning could easily induce draw resonance in the melt-spinning processing. Therefore, it is important to adjust processing condition and/or resin parameters to prevent tension-thinning and improve the spinnability of FEPs in fiber spinning or stretching. η_e of FEP is quite high, located from 7000 to 40,000 Pa s^{-1} in the tested σ_e range. It is known well that higher extensional viscosity would bring higher melt strength and thus better spinnability. η_e of FEP608 melt is higher than $3\eta_s$ at the same conditions, as depicted in Figure 5. Trouton ratio (μ, the ratio of extensional viscosity over shear viscosity) of FEP608 melt varies between 10 and 30, deviating far from Newtonian flow. Because of the narrow steady-state flow ranges, η_e of FEP600A and FEP600B are difficult to be calculated and not given in this article. It is noticeable that η_e of FEP is also higher than that of common polymers such as PE and PP,[19,35] and thus also better drawability.

Elasticity of FEP Melt

Elasticity plays an important role in polymer melts and can be estimated quantitatively by Bagley end correction and die swell. Usually, polymer melt elasticity would cause melt fracture. Recoverable shear deformation (S_R)[26,45] is used as an indicator for characterizing elasticity.

S_R can be calculated by Hilippoff and Gaskins's theory:[25]

$$e = e_c + S_R, \tag{5}$$

where e and e_c are the virtual ratio of length to diameter of capillary based on Bagley correction ($e = \frac{\Delta P_{ent}}{2\tau_a}$) and Couette correction, respectively. Although S_R is an elastic term, e_c is a viscous constant term at about 0.75. Hence, e is proportional to S_R, and it can be used to characterize polymer melt elasticity. The e values of FEP608 at different temperatures are shown in Figure 6. The results show that e values of FEP melts are rather low and even much lower than those of PP[35,37–38] and PS.[24] Meanwhile, with the increase of $\dot{\gamma}$, e of FEP608 first increases at low shear rate region, then followed by a plateau region. Finally, at the onset of unstable flow (the onset of stick-slip flow region), the plateau region drops abruptly and sharply. It suggests that wall-slip may begin and accumulated elastic energy is released. As elastic energy dissipation is facilitated at higher temperatures due to faster molecular motion, the elasticity of polymer melts at higher temperature is much lesser than that at lower temperatures. Figure 6 supports clearly this deduction. Of course, the elastic data, even those in plateau region, exist faint nonlinear feature due to the complexity of elasticity for polymeric materials.[41] Stable flow regions of FEP600B and 600A are too narrow to extract elasticity parameters.

Die swell is another way to characterize elasticity of polymer fluids. Die swell ratio (B) is the ratio of the equilibrium diameter of extrudates to the die diameter.[48] In this work, calculation of B is executed on an orifice die (polymer melt swelling is more obvious in orifice than that in long dies) and to avoid the shrinkage caused by cooling and/or crystallization via multiplying the density ratio between test temperature and room temperature.[35] The B

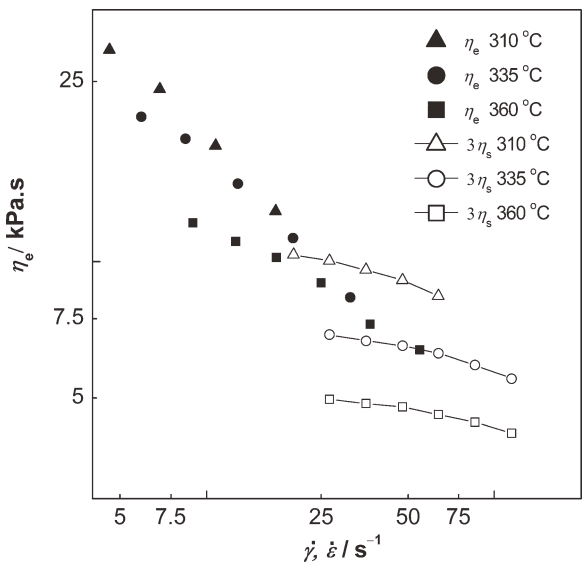

Figure 5 Comparison of extensional and shear viscosities for FEP608 at different temperatures.

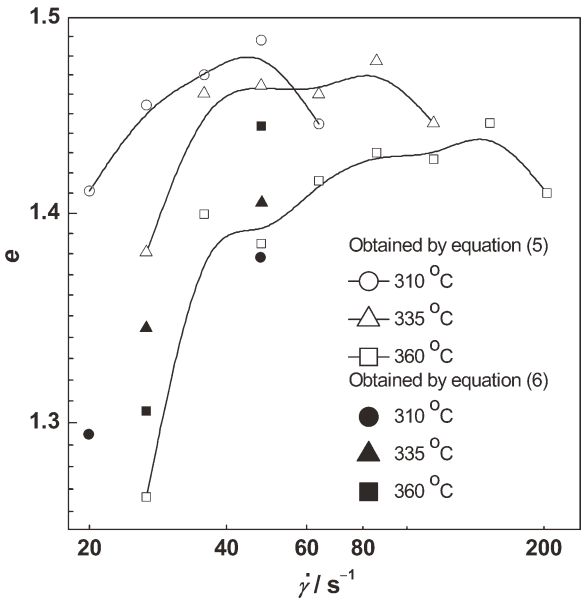

Figure 6 The virtual l/d ratio (e) of capillary based on Bagley correction for FEP608 at different temperatures.

values of FEP608 at three different temperatures are plotted as a function of $\dot{\gamma}$, as exhibited in Figure 7. Clearly, B increases with the increase of $\dot{\gamma}$ while less time is left to recover the elastic deformation in polymer extrudates.[27,45] The maximum B value of FEPs is around 2.14 at 1169 s^{-1} and 310°C, which is approaching to those of common polymers.[35,37–38,49] At higher processing temperatures, FEP melts relax more quickly and thus exhibit lower B values.[27,45] Figure 8 shows the plots of B versus $\dot{\gamma}$ at 360°C for three FEPs. It is found that the effect of MW on die swell is shear rate dependent. Although increased

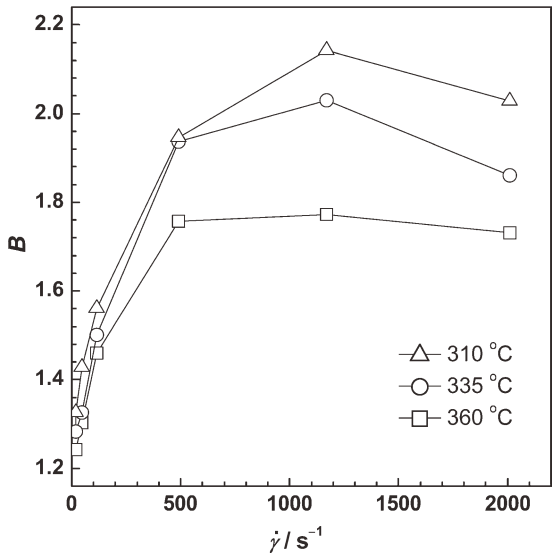

Figure 7 The die swell ratio B of FEP608 executed on an orifice die at different temperatures.

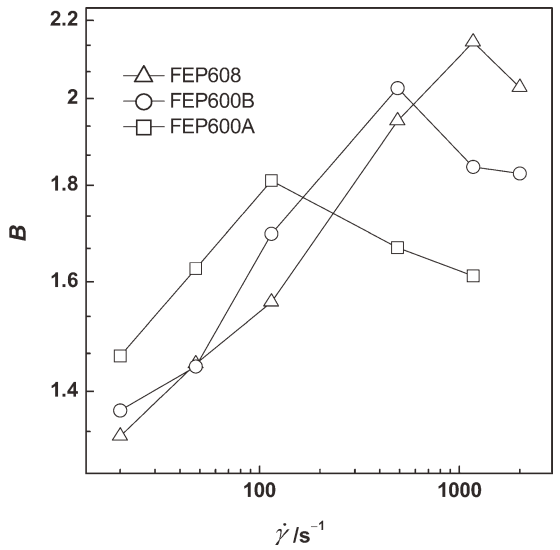

Figure 8 The die swell ratio B of three FEPs executed on an orifice die at 360°C.

MW affords bigger swell in stable flow region, it results in compressed die swell in the fracture regions. Therefore, FEP600A with the highest MW enjoys the highest B value in stable flow region but lowest in melt fracture regions.

To further confirm the accuracy of elasticity data in this study, above two elastic values were checked with the formula of Cogswell concerning recoverable shear deformation and die swell ratio[15]:

$$S_R = \ln B^2 \tag{6}$$

It is found that recoverable shear deformation values of FEP melt calculated from two expressions are almost equal [with the maximum difference of 0.12, tolerance of 10%, but only for the data obtained in steady flow region since eq. (6) does not work beyond this region, see Fig. 6], thus verified the correctness of the elasticity data.

Based on above evidences, it is possible to explain the poor processsability of FEP resins, namely their narrow stable flow region and remarkably early melt fracture. It is known that elasticity of polymer melts is the predominant cause of melt fracture. For FEP, although its melt elasticity is in the same level to those of common polymers, it holds distinct melt fracture phenomenon even at rather low flow rates, which is quite different from common polymers. Therefore, the elasticity does not account for the poor processability of FEP. However, high viscosity of FEP melt due to its stronger chain stiffness than common polymers (e.g., based on entanglement molecular weight evaluation, it can be derived that FEP possesses $\sim$ 918 C—C units[5] while that for PE is merely 107 units[42]) might act. The chain stiffness of FEP originates from larger size of F atom than H

atom and higher polarity of C—F bond than C—H bond. On one hand, larger atom size induces larger steric repulsions and thus less chain mobility for FEP than nonfluorinated polymers; on the other hand, higher polarity results in stronger coulomb repulsions and then bigger chain segments, complex helix conformation, thus less chain mobility of FEP.[6] Generally, polymer melts with high viscosity relax more slowly during extrusion. As a result, elastic energy is easy to accumulate and difficult to release even under fairly low shear rates, thus giving melt fractures in the remarkably early flow stage.

CONCLUSIONS

FEP melts hold five flow regions including stable region, sharkskin region, stick-slip region, super extrusion region, and gross distortion region. The stable flow region of FEP is quite narrow, causing poor processability. Shear and extensional rheology measurements of FEP melts under different temperatures were conducted. The Carreau model shows a good fit for the flow curve of FEP608 and η_0 was calculated to be 1.70 kPa s^{-1} at 360°C. And the extensional rheological data indicate that FEP resins have much lower *e* and *B* values when compared with those of common polymers, suggesting weaker elasticity during extrusion. Based on such rheological behaviors, the poor processability of FEP resins is ascribed to their high viscosity that originates from different molecular structure of fluoroploymer, which caused difficulties in chain movement and easily accumulated elastic energy.

Dongyue Group, Ltd. (P. R. China) is gratefully acknowledged for their kind offer of materials.

References

1. Zhang, Y.; Li, H.; Zhang, H. Fluorine-Containing Functional Materials (simplified Chinese); Chemical Industry Press: Beijing, 2008; Chapter 3.
2. Drobny, J. G. Technology of Fluoropolymers; CRC Press: London, 2000; Chapter 3.
3. Chen, W. C.; Lin, H. Y. Polym Bull 1996, 36, 51.
4. Ho, K.; Kalinka, G.; Tran, M.; Polyakova, N.; Bismarck, A. Compos Sci Technol 2007, 67, 2699.
5. Rosenbaoum, E. PhD Thesis, The University of British Columbia, 1998.
6. Ebnesajjad, S. Fluoroplastics, Volume 2—Melt Processible Fluoropolymers; Plastics Design Library: New York, 2000.
7. Wu, S. Macromolecules 1985, 18, 2023.
8. Tuminello, W. H. Polym Eng Sci 1989, 29, 645.
9. Kurose, T.; Takahashi, T.; Sugimoto, M.; Taniguchi, T.; Koyama, K. J Soc Rheol Jpn 2003, 31, 195.
10. Kurose, T.; Takahashi, T.; Nishioka, A.; Masubuchi, Y.; Takimoto, J.; Koyama, K. Rheol Acta 2003, 42, 338.
11. Rosenbaum, E.; Hatzikiriakos, S. AIChE J 1997, 43, 598.
12. Rosenbaoum, E.; Randa, S.; Hatzikiriakos, S.; Stewart, C.; Henry, D.; Buckmaster, M. Polym Eng Sci 2000, 40, 179.
13. Rosenbaoum, E.; Hatzikiriakos, S.; Stewart, C. Rheol Acta 1998, 37, 279.
14. Munstedt, H. J Rheol 1979, 23, 421.
15. Cogswell, F. N. Polym Eng Sci 1972, 12, 64.
16. Binding, D.; Walters, K. J Non-Newton Fluid Mech 1988, 30, 233.
17. Binding, D. M. J Non-Newton Fluid Mech 1988, 27, 173.
18. Binding, D. M.; Jones, D. M. Rheol Acta 1989, 28, 215.
19. Baldi, F.; Franceschini, A.; Riccò, T. Rheol Acta 2007, 46, 965.
20. Gotsis, A. D.; Odriozola, A. Rheol Acta 1998, 37, 430.
21. Padmanabhan, M.; Macosko, C. Rheol Acta 1997, 36, 144.
22. Laun, H. M.; Schuch, H. J Rheol 1989, 33, 119.
23. Shroff, R.; Cancio, L.; Shida, M. J Rheol 1977, 21, 429.
24. Thomas, D. P.; Hagan, R. S. Polym Eng Sci 1969, 9, 164.
25. Philippoff, W.; Gaskins, F. J Rheol 1958, 2, 263.
26. Han, C. D. Rheology in Polymer Processing; Academic Press: New York, 1976.
27. Larson, R. G. The Structure and Rheology of Complex Fluids; Oxford University Press: New York, 1999.
28. Haworth, B.; Gilbert, M.; Myers, D. J Mater Sci 2005, 40, 955.
29. Rosenbaoum, E. E.; Hatzikiriakos, S. G. AIChE J 1997, 43, 598.
30. Rosenbaoum, E. E.; Hatzikiriakos, S.; Stewart, C. Int Polym Proc 1995, 10, 204.
31. Kalika, D.; Denn, M. J Rheol 1987, 31, 815.
32. Li, H.; Hürlimann, H. P.; Meissner, J. Polym Bull 1986, 15, 83.
33. Vega, J.; Munoz-Escalona, A.; Santamaria, A.; Munoz, M.; Lafuente, P. Macromolecules 1996, 29, 960.
34. Delgadillo-Velázquez, O.; Georgiou, G.; Sentmanat, M.; Hatzikiriakos, S. Polym Eng Sci 2008, 48, 405.
35. Tao, Z.; Huang, J. Polymer 2003, 44, 719.
36. Barone, J.; Plucktaveesak, N.; Wang, S. J Rheol 1998, 42, 813.
37. Huang, J.; Tao, Z. J Appl Polym Sci 2003, 87, 1587.
38. Huang, J.; Leong, K. J Appl Polym Sci 2002, 84, 1269.
39. Ariawan, A.; Hatzikiriakos, S.; Goyal, S.; Hay, H. Adv Polym Tech 2001, 20, 1.
40. Vinogradov, G.; Malkin, A. Rheology of Polymers: Viscoelasticity and Flow of Polymers; Mir Moscow, 1980.
41. Liang, J. Polym Test 2004, 23, 441.
42. Tuminello, W. H.; Treat, T. A.; English, A. D. Macromolecules 1988, 21, 2606.
43. Zen, J.; Li, Y.; He, J. Acta Polym Sin 2000, 1, 69.
44. Gupta, R. Polymer and Composite Rheology; CRC, 2000.
45. Ferry, J. D. Viscoelastic Properties of Polymers; Wiley, 1980.
46. Nguyen, T.; Kausch, H. Colloid Polym Sci 1991, 269, 1099.
47. Chen, K.; Shen, J.; Tang, X. J Appl Polym Sci 2005, 97, 705.
48. Rough, S.; Wilson, D. J Mater Sci 2005, 40, 4199.
49. Liang, J. J Thermoplast Compos Mater 2009, 22, 99.